Tree Physiology 34, 285–301
doi:10.1093/treephys/tpu009

Research paper

Transpiration characteristics of a rubber plantation in central Cambodia

Nakako Kobayashi[1,8], Tomo'omi Kumagai[1], Yoshiyuki Miyazawa[2], Kazuho Matsumoto[3], Makiko Tateishi[4], Tiva K. Lim[5], Ryan G. Mudd[6], Alan D. Ziegler[7], Thomas W. Giambelluca[1,6] and Song Yin[5]

[1]Hydrospheric Atmospheric Research Center, Nagoya University, Furo-cho, Chikusa-ku, Nagoya, Aichi 464-8601, Japan; [2]Research Institute for East Asia Environments, Kyushu University, Motooka, Fukuoka 811-0395, Japan; [3]Faculty of Agriculture, University of the Ryukyus, Chihara, Okinawa 903-0213, Japan; [4]Faculty of Agriculture, Kyushu University, Sasaguri, Fukuoka 811-2415, Japan; [5]Cambodian Rubber Research Institute, Phnom Penh, Cambodia; [6]Department of Geography, University of Hawai'i at Mānoa, Honolulu, HI 96822, USA; [7]Faculty of Arts and Social Sciences, National University of Singapore, Lower Kent Ridge Road, Singapore 119077, Singapore; [8]Corresponding author (naka-koba@nagoya-u.jp)

Received April 26, 2013; accepted January 26, 2014; published online March 18, 2014; handling Editor David Whitehead

The rapid and widespread expansion of rubber plantations in Southeast Asia necessitates a greater understanding of tree physiology and the impacts of water consumption on local hydrology. Sap flow measurements were used to study the intra- and inter-annual variations in transpiration rate (E_t) in a rubber stand in the low-elevation plain of central Cambodia. Mean stand sap flux density (J_S) indicates that rubber trees actively transpire in the rainy season, but become inactive in the dry season. A sharp, brief drop in J_S occurred simultaneously with leaf shedding in the middle of the dry season in January. Although the annual maxima of J_S were approximately the same in the two study years, the maximum daily stand E_t of ~2.0 mm day^{-1} in 2010 increased to ~2.4 mm day^{-1} in 2011. Canopy-level stomatal response was well explained by changes in solar radiation, vapor pressure deficit, soil moisture availability, leaf area, and stem diameter. Rubber trees had a relatively small potential to transpire at the beginning of the study period, compared with average diffuse-porous species. After 2 years of growth in stem diameter, transpiration potential was comparable to other species. The sensitivity of canopy conductance (g_c) to atmospheric drought indicates isohydric behavior of rubber trees. Modeling also predicted a relatively small sensitivity of g_c to the soil moisture deficit and a rapid decrease in g_c under extreme drought conditions. However, annual observations suggest the possibility of a change in leaf characteristics with tree maturity and/or initiation of latex tapping. The estimated annual stand E_t was 469 mm year^{-1} in 2010, increasing to 658 mm year^{-1} in 2011. Diagnostic analysis using the derived g_c model showed that inter-annual change in stand E_t in the rapidly growing young rubber stand was determined mainly by tree growth rate, not by differences in air and soil variables in the surrounding environment. Future research should focus on the potentially broad applicability of the relationship between E_t and tree size as well as environmental factors at stands different in terms of clonal type and age.

Keywords: canopy conductance, canopy transpiration, environmental control, *Hevea brasiliensis*, sap flow.

Introduction

The rubber tree (*Hevea brasiliensis* Müll. Arg.) is native to the tropical rain forests of Amazonia. Rubber seedlings were introduced into Southeast (SE) Asia in the 1870s by the British (Priyadarshan 2011). Rubber has now expanded throughout this region as a cash crop. The rubber harvesting area in SE Asia was ~7.0 Mha in 2010, and it accounted for 75% of the world total (FAO 2010). The highest production is in Thailand, followed by Indonesia, Malaysia, Viet Nam, the Philippines, Myanmar and Cambodia. A substantial amount of rubber is also grown in areas

of southern China (Qiu 2009, Li and Fox 2012). The optimal growing conditions are the following: 2000–4000 mm rainfall without a dry season; a mean annual temperature of 28 ± 2 °C; and sunshine hours of ~2000 h year^{-1}, distributed fairly equally in all months (Priyadarshan 2011). While many of these areas are suitable for rubber cultivation, others are marginal, having about half of the year with near-ideal conditions, but other months with stressful conditions including low or high temperature or near-drought conditions. Recent aggressive breeding programs have succeeded in producing rubber clones that are tolerant to relatively cold and dry environments with little effects on latex productivity (Priyadarshan 2003). The demonstrated success of rubber plantations in regions previously thought to be unsuitable for rubber production and the increasing demand for natural rubber from developing countries are currently promoting further expansion of rubber cultivation.

As discussed by Kumagai et al. (2013), rubber cultivation has positive and negative societal and environmental implications. It provides for the livelihoods of smallholders and their workers, together numbering in the millions (Simien and Penot 2011), and acts as a carbon sink in the case of conversion from non-forested areas (Wauters et al. 2008). However, some concerns about the rubber expansion in montane mainland SE Asia have been expressed (e.g., Wu et al. 2001, Qiu 2009, Ziegler et al. 2009). Several possible negative environmental consequences have been cited: e.g., decrease in biodiversity, reduction of total carbon biomass, acceleration of erosion and surface runoff, and stream desiccation caused by the reduced infiltration capacity in managed soils and high water consumption by rubber trees. Understanding the hydrological characteristics of rubber plantations is crucial for their sustainable management. In an initial analysis conducted in Xishuangbanna Prefecture in southern China, Guardiola-Claramonte et al. (2008) showed depletion in deep-layer soil moisture due to water uptake by rubber trees at the end of the dry season, after leaf flush but before the beginning of the rainy season. Simulation results suggested that widespread increases in water loss through evapotranspiration could occur by replacing traditional vegetation cover by rubber trees (Guardiola-Claramonte et al. 2010). Recently, Tan et al. (2011) alleged that rubber plantations acted as 'water pumps' compared with nearby rain forests based on eddy covariance measurements, and the results were validated by catchment water balance. Although high water consumption is suspected to be a trait of rubber trees, it has not been shown with certainty because of a lack of knowledge about the partitioning of evapotranspiration into water flux components in plantations, i.e., soil evaporation, transpiration of trees and understory vegetation, and evaporation from a wet canopy.

Tree transpiration often accounts for a large portion of evapotranspiration (E) in tree-dominated stands, e.g., transpiration made up ~50% of E in a temperate mixed deciduous forest (Wilson et al. 2001) and 65% of E in a Dahurica larch (*Larix gmelinii* Rupr.) forest (Ohta et al. 2001). Because transpiration is strongly dependent on stomatal control (Jarvis and McNaughton 1986), the physiological characteristics of different tree species are important in determining their water use. Numerous studies have been conducted on rubber physiology (Priyadarshan 2011). Many have focused on relationships of latex production or tree growth with environmental conditions (e.g., Rao et al. 1990, Ranasinghe and Milburn 1995, Vijayakumar et al. 1998, Senevirathna et al. 2003). Sufficient study of the transpiration rates (E_t) of rubber trees is, however, critically lacking for deriving reliable physiological parameters, which are required in eco-hydrological models to constrain stomatal response to environmental factors. Recent results of E_t in a stand of rubber trees growing in northeast Thailand based on sap flow measurements (Isarangkool Na Ayutthaya et al. 2011) indicated only a moderate level of water consumption, which was not as high as expected for a tree crop growing in the tropics (Carr 2012). They also found isohydric behavior of rubber trees under intermittent drought in the rainy season, and introduced a simple hydraulic model to simulate tree E_t. However, the applicability of the results for wide atmospheric-soil conditions and different rubber clones is uncertain, and longer-term continuous measurements of E_t in varied environments are still necessary to define the physiological behavior of rubber tree plantations.

Most prior studies concerning rubber–water relations at stand or larger scales have been conducted in southern China or northern Thailand, which are non-traditional/marginal areas for rubber cultivation (Priyadarshan 2003). Our group has been conducting sap flow measurements at a rubber plantation in central Cambodia since the beginning of 2010. This region is categorized as a traditional area (Li and Fox 2012). Although the area under rubber cultivation in Cambodia is much smaller than in major producing countries such as Thailand or Indonesia, Cambodia plans dramatic increases in rubber cultivation following the lead of neighboring countries (Li and Fox 2012). The goal of our study was to understand the level of water consumption and the physiology of rubber trees under typical rubber growing conditions at a site in Cambodia using sap flow observations during 2 years (2010–2011). The measurements were complemented with simultaneous measurements of micrometeorology, including turbulent fluxes by the eddy covariance method on a co-located observation tower. The rubber plantation study site, located in a low-elevation, low-relief area along the Mekong river, was selected because of its suitability for investigating one-dimensional water budgets.

Materials and methods

Site description

The measurements were carried out in a 725-ha brevi-deciduous rubber plantation in Kampong Cham Province,

Cambodia (11°57′N, 105°34′E, ~50 m above sea level) beginning in January 2010. The plantation is underlain by basaltic latosols. The clay-rich soil contained 8.4% fine sand, 10.1% coarse silt, 19.5% fine silt and 55.1% clay. Regional climate is tropical savanna (Aw) according to Köppen's classification. The local climatology is not known in detail because long-term observations are not available. Based on the data summarized in 'The Atlas of Cambodia: National Poverty and Environment Maps' (SCW 2006), annual mean temperature and rainfall are 27.1 °C and 1694 mm at the Kampong Cham station, located 12.5 km WNW of the site. Based on data measured in a clearing within the plantation <1 km from the study site, the 10-year (2000–2009) mean annual precipitation was 1398 mm, with a minimum of 986 mm in 2004 and a maximum of 1678 mm in 2008. The climate is governed by the Asian monsoon regime, which produces two distinct seasons: a rainy season from May to October and a dry season from November to April.

Several experimental plots in the study rubber plantation differing in breed, age and planting design are managed by the Cambodian Rubber Research Institute (CRRI). In our sample plot, rubber trees were grown under rainfed conditions, and all trees were clone RRIC 100 planted in 2004 with a nearly regular spacing of 6 m in the north–south direction and 3 m in the east–west direction (Table 1). The stand planting density was 555 trees ha^{-1}, but 17.5% of the trees died before reaching maturity. Tree size measurements were conducted for 98–99 trees in the early part of each year. The mean canopy height of 11.4 m in February 2010 increased to 12.9 m in March 2011, and reached 14.3 m in March 2012. The crown space was limited to the upper 3–4 m, below which a trunk space was found with few branches. Moderately dense understory vegetation consisted of various species of herbaceous plants and shrubs. Larger stems were occasionally cut to limit competition with rubber trees.

Table 1. Stand characteristics of the studied rubber plot. Tree height and stem diameter were measured for 98 to 99 trees. The range of the values results from both the annual cycle and inter-annual variability during the period February 2010 through March 2012.

Characteristic	
Plot area (m^2)	2160
Age (years)	7–8
Density[1] (trees ha^{-1})	458
Leaf area index[2]	0.8–5.0
Mean stem diameter[3] (m)	0.133–0.160
Basal area (m^2 ha^{-1})	6.5–9.4
Sapwood area[4] (m^2 ha^{-1})	5.6–8.3
Mean tree height (m)	11.4–14.3
Sap flux measurements (trees)	10

[1]Although planting density was 555 trees ha^{-1}, the tree mortality was 17.5% in the study plot by the time of the study.
[2]Leaf area index was measured by LAI-2000 or LAI-2200 at irregular intervals.
[3]Stem diameter was measured at 1.7 m to avoid the tapping cut.
[4]Total sapwood area was assumed to be equivalent to basal area, but slightly reduced for bark of ~5-mm thickness.

Stem diameter and leaf area index

The mean stem diameter (hereafter referred to as d), which was measured above the tapping zone at 1.7-m height above the ground, was 0.133 m ($\sigma = 0.0225$ m, $n = 98$, where σ is the standard deviation and n is the sample size) in 2010, 0.153 m in 2011, and 0.160 m in 2012 (Figure 1). Outside of the plot but within the same stand, d was measured at biweekly or monthly intervals for 137 sample trees. To obtain a smooth growth curve of the mean d, the annual observation in the study plot mentioned above was interpolated based on the pattern of the more frequently observed adjacent plot. The whole-canopy leaf area index (L_c) value, which was measured by a plant canopy analyzer (LAI-2000 or LAI-2200, LI-COR, Lincoln, NE, USA) at 5-m intervals along a diagonal transect, reached a maximum of 4–5 in summer (July–September), and leaf abscission dramatically increased in the beginning of January, making way for new leaves, which emerged near the end of January in both years. The L_c measurements were conducted eight times in 2010 and twice in 2011. Because the measurements in 2011 were scarce, seasonal variation was estimated based on the measured value near the time of maximal L_c in August 2011 and on the annual cycles of 2010 and 2012. Additionally, the timings of leaf fall and leaf area recovery were estimated based on albedo measurements and visual observations by CRRI staff.

Meteorological measurements

Four components of net radiation (R_n), air temperature (T_a) and humidity were measured with a net radiometer (NR01,

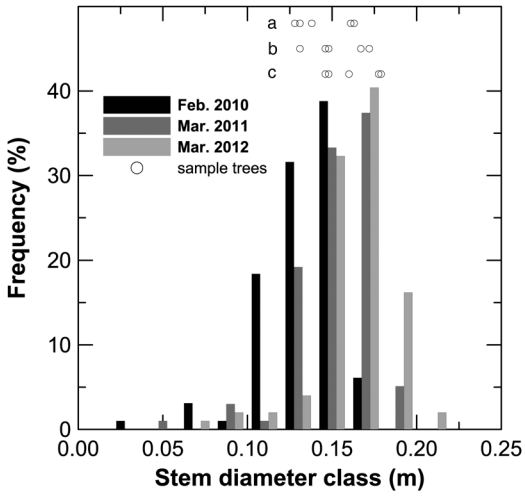

Figure 1. Frequency distribution of stem diameters in the study plot. The values were measured at 1.7-m height above the ground (to avoid the tapping cut) for 98–99 trees in the early part of each year. Trees sampled for sap flow were changed for the three periods (a, January–August 2010; b, August 2010–August 2011; c, August–December 2011).

Hukseflux Thermal Sensors, Delft, The Netherlands) and a thermohygrometer (HMP45D, Vaisala, Helsinki, Finland), respectively, installed at a height of 30 m above the ground. At approximately the same height, three-dimensional wind velocity and sonic temperature were measured with a three-dimensional sonic anemometer (CSAT3, Campbell Scientific, Inc., Logan, UT, USA), and used to derive mean wind speed (U), friction velocity (u_*) and turbulent sensible heat flux (H). Samples were taken every 0.1 s and averaged over 30 min (CR3000, Campbell Scientific). Two rain gages (TE-525, Texas Electronics, Inc., Dallas, TX, USA) installed at a height of 15 m (near the top of the canopy to reduce the wind measurement error) were used to obtain precipitation rate (P_r). Soil heat flux (G) was estimated as the average of measurements of four soil heat plates buried at 0.08-m depth (HFP01, Hukseflux Thermal Sensors). Volumetric soil moisture content (θ; $m^3\ m^{-3}$) was measured with amplitude domain reflectometry sensors (ThetaProbe, Delta-T Devices Ltd, Cambridge, UK) at 0.05, 0.1, 0.2, 0.3 and 0.5 m below the forest floor. The missing soil moisture values for 73 days were interpolated by supplementary observations at 0.04-m and 0.35–0.65-m depths using time domain reflectometry (TDR) sensors (CS616, Campbell Scientific). Soil moisture content was also monitored in 1.05–1.35, 2.03–2.33, and 3.08–3.38 m soil layers with the TDR sensors installed vertically. The P_r, G, and soil moisture data were taken at 30-s intervals and averaged over 30 min (CR23X and CR1000, Campbell Scientific).

The weighted average of θ in the 0–0.5 m soil layer was calculated as $\theta_{0-50} = (7.5\theta_5 + 7.5\theta_{10} + 10\theta_{20} + 15\theta_{30} + 10\theta_{50})/50$, where the subscripts denote measurement depth (cm) below ground level. The relative extractable water in the soil (Θ; $m^3\ m^{-3}$) was calculated as $\Theta = (\theta_{0-50} - \theta_r)/(\theta_f - \theta_r)$, where θ_f and θ_r are the water content at field capacity and the residual water content averaged in the 0–0.5-m layer, respectively. Although the Θ was obtained from a single θ profile in the study plot, its representativeness was supported by a second Θ time series based on a θ profile in the neighboring plot, ~60 m from the study plot. Maximum and minimum daily mean values of θ_{0-50} observed during the 2 years were assigned to θ_f and θ_r (0.384 and 0.215, respectively). Based on these values, the estimated available water capacity at the site is moderate.

Sap flux measurements

Xylem sap flux density (F_d) measurements were conducted by the thermal dissipation method with Granier-type sensors (Granier 1987). Each sensor consisted of a pair of probes 20 mm long and 2 mm in diameter. The two probes were installed above the tapping cut, at 1.7-m height above the ground, into the sapwood ~0.15 m apart from each other in the vertical direction. The upper probe included a heater supplied with 0.2-W constant power. The temperature difference between the upper heated probe and the lower unheated reference probe was then measured and converted to F_d according to the method of Granier (1987). Because rubber trees have diffuse-porous wood, the use of Granier's empirical equation is appropriate (Clearwater et al. 1999). Sap flow signals were scanned every 30 s and recorded as 30-min averages on a data logger (CR1000) with a multiplexer (AM16/32, Campbell Scientific). A total of 10 trees were selected to measure F_d. In five of the trees (Group A), two sensors were installed in each tree in the outer 20 mm of the sapwood after removing the bark (5-mm thickness) to capture tree-to-tree variation in F_d. In the other five trees (Group B), four sensors were installed at xylem depths of 0–20, 20–40 and 40–60 mm, to measure the radial variation in F_d over the entire sapwood thickness. Two sensors for the 0–20-mm depth were placed on the north- and south-facing side of the trees, and the sensors for 20–40 and 40–60-mm depths were placed on the east- or west-facing side of the trees.

Breaking of sap flow sensors was very frequent because of high activity of ants and mice. Furthermore, tree growth was so rapid that the sensors often broke within a few months, and if they did not break they were gradually pushed out of the xylem. For these reasons, frequent reinstallation of the sensors was necessary, and trees were somewhat damaged after periods of several months to a year of study. We therefore changed sample trees frequently to reduce the influence of damage on the measurements (see Figure 1). For instances when the power circuit was broken but the thermocouple circuit remained intact, the resulting data allowed us to evaluate the natural temperature gradient (ΔT_{nat}) between the two probes. Although each trunk where the sensors were installed was insulated to shield it from direct radiation, the ΔT_{nat} affected the measurements, probably because of the heat transfer from the well-lit forest floor below the canopy with inter-row gaps.

The ΔT_{nat} was not negligible in the trees of Group B, sometimes reaching ±1 °C, and the error was more pronounced for the sensors installed at xylem depths deeper than 20 mm. A likely reason for the occurrence of larger ΔT_{nat} in Group B compared with Group A was that two heated probes at different depths (0–20 and 20–40 mm, or 0–20 and 40–60 mm) were paired with an unheated reference probe at the middle of the depths to save probes as well as to prevent trees from excess damage. In other words, the time lag of the heat transfer from the stem surface to the reference and heated probes located at different depths may have caused the larger ΔT_{nat}. The ΔT_{nat} values observed in the trees of Group A were generally small (±0.3 °C). These tended to become large at the second half of the dry season when foliage was sparse and the diurnal range of air temperature was relatively large. The influence of ΔT_{nat} on daily mean F_d was estimated to be < ± 15% in Group A, while it reached 27% in Group B. The errors for Group A were similar in magnitude to the tree-to-tree variation, and appeared in both

positive and negative directions, indicating that it would affect mean sap flux density to only a limited extent. Therefore, only the data of Group A were used in our final estimates of transpiration. However, Group B data were used to confirm seasonal patterns.

Calculation of transpiration rate

Mean stand sap flux density (J_S) is generally calculated from F_d measured at all depths in an adequate number of sample trees, taking into account radial variation in F_d (see Kumagai et al. 2005, 2007). Because high ΔT_{nat} values were observed in sap flow data of Group B, radial patterns in F_d obtained with Group B data were not considered reliable in the present study. Using the transient thermal dissipation method established to address the issue of natural temperature gradient, Isarangkool Na Ayutthaya et al. (2010) have determined the radial patterns for rubber trees, with F_d at a maximum in the outer ring and becoming smaller toward the center. They derived a reduction coefficient of 0.874 for the F_d in the outermost ring (F_{d_out}) to determine the mean F_d value in a whole tree. Their rubber trees are similar to ours in age and diameter: a few years older and a few tens of millimeters thicker. A similar coefficient was supported by the study of Phillips et al. (1996), who showed an insignificant radial change of F_d in diffuse-porous species. Therefore, J_S was calculated by simply applying the 0.874 coefficient to the value measured at the 0–20 mm depth:

$$J_S = 0.874 \frac{\sum_{i=1}^{n} A_{S,i} F_{d\_out,i}}{\sum_{i=1}^{n} A_{S,i}} \quad (1)$$

where n is the sample size and $A_{S,i}$ is the total sapwood area for individual tree i. Here, the $F_{d\_out,i}$ value was calculated as an average of two measurements on the south- and north-facing side. If either one was missing, the other was used alone. In general, the F_{d_out} value on the south side was larger than the value on the north side; the difference was small, ~5%, on average.

Before estimating stand J_S, the adequacy of the sample size should be examined. A relationship between sample size and coefficient of variation (CV) of J_S was estimated by Monte Carlo analysis following Kumagai et al. (2007). In this analysis, F_{d_out} values observed in the trees of Group B (see Sap flux measurements section) were temporarily included to increase the total sample size. According to Čermák et al. (2004), a minimum scaling-up error of 5–10% can be expected using reasonable sets of sample trees in homogeneous stands. Using the data of 39 days when daily mean F_{d_out} values were obtained in all of 10 sample trees, the CV values calculated for the study rubber stand averaged 10% when the sample size was five (Figure 2). The minimum necessary sample size was apparently smaller than in previous

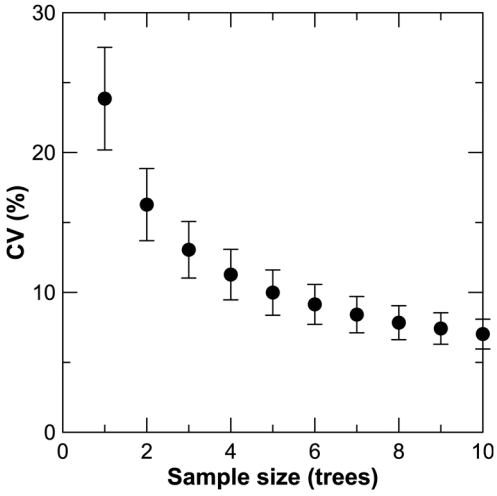

Figure 2. Relationship between sample size and the CV of daily integrated mean stand sap flux density (J_S). Symbols and error bars indicate averages and standard deviations of CVs, respectively, over 39 days when xylem sap flux densities at a depth of 0–20 mm (F_{d_out}) were obtained in all of 10 sample trees.

studies: 10 trees in Japanese cedar (*Cryptomeria japonica* D. Don) stands (Kumagai et al. 2007) and 15 trees in a Japanese cypress (*Chamaecyparis obtusa* (Sieb. et Zucc.) Endl.) plantation (Kume et al. 2010). However, the size distribution in those studies was wider than for the rubber stand; the differences between the minimum and maximum d values for the cedar stands were 0.20 and 0.32 m, and for the cypress stand it was 0.24 m, while that of the study rubber stand was only 0.10–0.12 m, with the exception of one tree, which was planted to replace the one that died (see Figure 1). The small minimum necessary sample size is not surprising for a systematically planted clonal rubber stand. Given that the CV value calculated from only F_{d_out} values that were not affected by ΔT_{nat} errors would be smaller than this value, four was accepted as the minimum necessary sample size.

Next, the half-hourly J_S values were integrated over one full day (0500–0500 local time (LT)). This manipulation enabled us to assume the effect of stem water capacitance to be small, and to regard sap flux density as tree transpiration. The daily integrated stand E_t was then calculated as

$$E_t = J_S \frac{A_S}{A_G} \quad (2)$$

where A_S and A_G are the total sapwood area and ground area, respectively, in the study plot. Isarangkool Na Ayutthaya et al. (2010) conducted cut stem experiments for rubber trees, confirming that the whole xylem area was completely conductive, except for thin piths. Because our rubber trees were younger than theirs by a few years, similar conditions could be reasonably expected. Thus, we assumed that $A_{S,i}$ was equivalent to the tree basal area, which was computed from measured d, slightly reduced for bark of ~5-mm thickness. The A_S value

was calculated in the same manner, but with the mean stand d. Because of the small variation in d among individual trees, using the mean d to calculate A_S differed only slightly from the sum of $A_{S,i}$.

Calculation of canopy conductance

Canopy conductance (g_c) was calculated from inversion of the following equation:

$$E_t = \rho \frac{g_a g_c}{g_a + g_c}\left[q_{sat}(T_s) - q\right] \quad (3)$$

where ρ is the density of air, q the specific humidity, T_s the canopy surface temperature, g_a the aerodynamic conductance for water vapor transfer, and the subscript sat refers to saturated conditions. Units for g_c were converted from mm s^{-1} to mmol m^{-2} s^{-1} by multiplying by a factor of 41 (for 25 °C) following Oren et al. (1999). Note that g_c was calculated as a daytime mean, and data for rainy days and when the vapor pressure deficit $D < 0.1$ kPa were not included (see Phillips and Oren 1998). For this calculation, independent variables in Eq. (3) were averaged for daylight hours (0630–1730 LT). The daytime mean stand E_t was calculated by dividing daily integrated stand E_t by the number of daylight hours, following Phillips and Oren (1998). The day length did not change with seasons (variance was always within 10%).

Here, g_a was calculated on the basis of the traditional Monin–Obukhov similarity theory by the following equation (cf. Kobayashi et al. 2007):

$$g_a = \frac{k^2 U}{\left[\ln(z/z_0) - \Psi_m(\zeta) + \Psi_m(\zeta_0)\right]\left[\ln(z/z_t) - \Psi_h(\zeta) + \Psi_h(\zeta_t)\right]} \quad (4)$$

where k is von Kármán's constant (0.4), ζ atmospheric stability (z/L, where z is the height above the displacement height and L is the Obukhov length), and z_0 and z_t are roughness lengths for momentum and heat transfer, respectively. The parameters ζ_0 and ζ_t are defined as z_0/L and z_t/L, respectively, Ψ_m and Ψ_h are the integral universal stability correction functions (Brutsaert 1999, Cheng and Brutsaert 2005), and the subscript m stands for momentum and h for heat transfer. The value of displacement height was set to 3/4 of the mean tree height as a typical value for forest according to Kaimal and Finnigan (1994). The value of z_0 was estimated from the equation of the logarithmic wind profile under near-neutral conditions, which averaged 1.74 m. Because an increasing trend of z_0 was observed with time, probably due to increasing tree height, a linear relationship between monthly mean z_0 and the number of days since the start of the analysis was applied to calculation of g_a. The value of z_t was calculated by assuming a parameter kB^{-1}, the logarithm of the ratio between z_0 and z_t, to be a typical value of 2.0 (Mölder and Lindroth 2001). Note that half-hourly data of ζ often showed outliers, and thus the daytime mean values were recalculated using the daytime mean u_*, H and other constituent variables. The effective surface temperature for sensible heat was estimated from the calculated g_a, H and T_a, and it was substituted for T_s in computing $q_{sat}(T_s)$.

To derive physiological parameters from sap-flow-derived g_c, multiplicative-type functions of downward shortwave radiation (S_d), vapor pressure deficit D, relative extractable water in the soil Θ, air temperature T_a, and leaf area index L_c (e.g., Jarvis 1976) were used following Granier and Bréda (1996), with some modifications described below, as:

$$g_c = g_{cref} f_1(S_d) f_2(D) f_3(\Theta) f_4(T_a) f_5(L_c) \quad (5)$$

$$f_1(S_d) = \frac{S_d}{S_d + \alpha} \quad (6)$$

$$f_2(D) = 1 - \beta_1 \ln D \quad (7)$$

$$f_3(\Theta) = 1 + \beta_2 \log_{10}\Theta \quad (8)$$

$$f_4(T_a) = \left(\frac{T_a - T_{min}}{T_{opt} - T_{min}}\right) \times \left(\frac{T_{max} - T_a}{T_{max} - T_{opt}}\right)^{\left(\frac{T_{max} - T_{opt}}{T_{opt} - T_{min}}\right)} \quad (9)$$

$$f_5(L_c) = 1 - e^{-\beta_3 L_c} \quad (10)$$

where g_{cref} is a reference value of g_c under non-limiting conditions (e.g., high irradiance, adequate soil water, optimal air temperature T_{opt}, and mature foliage) at $D = 1$ kPa, and the units of g_c and g_{cref} are mmol m^{-2} s^{-1}. The values of T_{max} and T_{min} were defined as 50 and 10 °C, respectively. Eq. (10) represents an increase in g_c with increasing L_c as well as leaf maturity.

For rapidly growing trees such as young rubber, sapwood area A_S is an important variable in the g_c estimation. The E_t value is a multiple of A_S according to Eq. (2). Given that g_a is sufficiently larger than g_c in Eq. (3), i.e., strong coupling between conditions at the leaf surface and those in the air outside the leaf boundary layer, fractional change in E_t would cause an equal fractional change in g_c (Jarvis and McNaughton 1986). In other words, g_c would be linearly related to A_S. However, because it is highly conceivable that partial decoupling from the atmosphere occurs in broad-leaved stands such as a rubber plantation, a fractional change in E_t would cause a larger fractional change in g_c. Alternatively, an increase in A_S is generally associated with an increase in tree height, a factor that might increase the xylem resistance for water movement. Larger xylem resistance would result in smaller J_S, and thus smaller g_c as shown by Schäfer et al. (2000). Furthermore, assuming that the growth of aboveground biomass is accompanied by an increase in belowground biomass, root development in vertical as well as horizontal directions was possible. This might increase the ability of the trees to tap soil water.

Although the three factors mentioned above were considered to be minor compared with the increase in conductive xylem area for the change in g_c, we applied a power function to represent the effect of tree growth on g_c, combining these effects together. The effect of tree growth was included into the g_{cref} value as follows:

$$g_{cref} = g_{cref0} f_6(c_r) \quad (11)$$

$$f_6(c_r) = c_r^{\beta_4} \quad (12)$$

where c_r represents the A_S factor, which is defined as $(d/d_0)^2$. Here, the subscript zero denotes the corresponding value on 1 January 2010. When β_4 is close to one, g_{cref} is linearly related to A_S, indicating that contribution of the other factors is negligible. Referring to the response functions above, $f_2(D)$ and $f_6(c_r)$ range higher than one, in contrast to the other functions, which range from zero to one.

The symbols g_{cref0}, α, β_1, β_2, β_3, β_4, and T_{opt} are the fitting parameters to be estimated through non-linear multiple regression analysis, which was carried out using the MATLAB software (MathWorks, Inc., Natick, MA, USA).

Potential evapotranspiration rate

The potential evapotranspiration rate (E_p) refers to the evapotranspiration rate from a large uniform vegetated surface with sufficient available moisture (Brutsaert 1982). The E_p value was calculated on a daily basis using the Penman (1948) equation with the original empirical wind function as follows:

$$E_p = \frac{\Delta}{\Delta+\gamma}\frac{(R_n - G)}{\lambda} + \frac{\gamma}{\Delta+\gamma} f(U) D \quad (13)$$

where Δ is the slope of the saturation vapor pressure versus temperature curve, γ the psychrometric constant, λ the latent heat for vaporization and $f(U) = 0.26\ (1 + 0.54U)$. Originally, the relationship was derived using U at the level of 2 m above the surface. Penman E_p is more applicable to open water surfaces and natural land covers with low roughness than to high-roughness land covers such as tree plantations. Nevertheless, it is widely used in hydrological practice, and serves our purpose to show the seasonal pattern of evaporative demand at the study site.

Results

Meteorological conditions and stand biometric parameters

Distinct seasonal changes in several meteorological variables and biometric parameters can be seen in the 2010–2011 time series (Figure 3). The rainfall events were concentrated between April and October, with a marked dry season in between

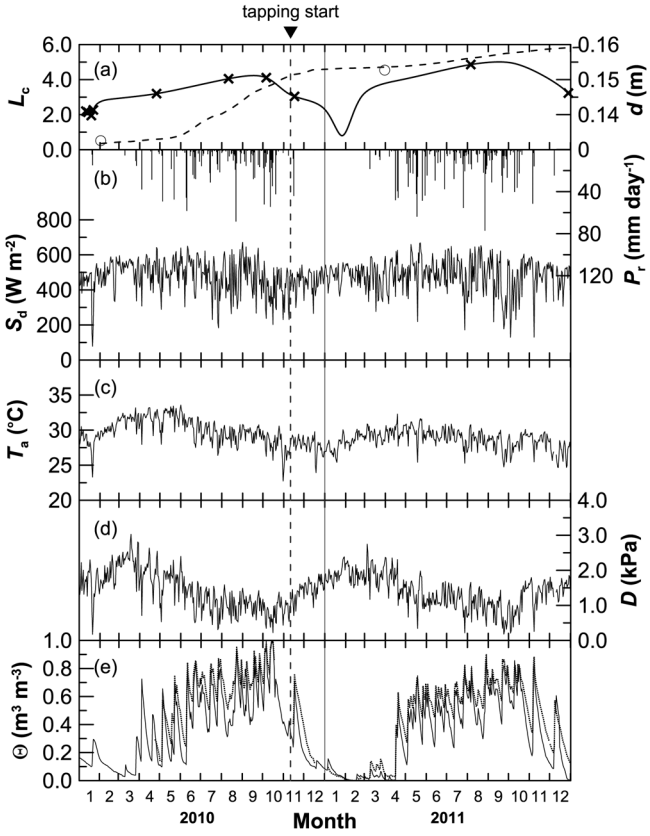

Figure 3. Meteorological data and stand biometric parameters obtained at the study site during 2010–2011. (a) Canopy leaf area index (L_c; crosses with solid line, left scale) and mean diameter at breast height (d; open circles with dotted line, right scale), (b) downward shortwave radiation (S_d; thin line, left scale) and daily precipitation (P_r; bars, right scale), (c) air temperature (T_a), (d) vapor pressure deficit (D) and (e) relative extractable water in the 0–0.5-m soil layer (Θ) for the study plot (solid line) and for a neighboring plot (dotted line). All atmospheric conditions were measured above the canopy, and are represented as daytime means except for daily sums of P_r. For L_c and d, symbols and lines indicate measurements and interpolated trends, respectively (see the details in Stem diameter and leaf area index section). The vertical lines represent the start of the year 2011 (solid) and the start of tapping (dotted).

(Figure 3b). The annual precipitation rate P_r was smaller in 2010 (1332 mm year^{-1}) than in 2011 (1545 mm year^{-1}); the annual mean T_a was higher in 2010 (28.0 °C) than in 2011 (27.0 °C). In light of the climatology mentioned in the section Site description, the weather conditions in 2010 were characterized by dry and hot conditions relative to the mean. In contrast, the weather conditions in 2011 were close to normal despite heavy flooding throughout many areas of mainland SE Asia. The months of January–March were not as dry and the pre-monsoon rains started earlier in 2010 compared with 2011 (Figure 3b and e). However, rain events occurred very infrequently through the months of April–May, resulting in an extended period of water-limited conditions for early 2010. Around the same period (February–May), T_a was comparatively higher in 2010 than in the following year, and consequently D was larger (Figure 3c and d).

Growth in stem diameter d was observed in the rainy season of both years (Figure 3a), and the rate was remarkably higher in 2010 (0.022 m year^{-1}) than in 2011 (0.006 m year^{-1}). The maximal leaf area index L_c was slightly larger in 2011 (~5.0) compared with 2010 (~4.1), as expected with the continuing maturation of the stand. In 2010, a significant portion of leaves on lower branches remained on the trees until May or June, while in 2011, all old leaves on the lower branches dropped within a few weeks after leaf flush around the end of January.

Transpiration rate at individual tree and stand scale

Seasonal patterns in daily mean F_{d_out} were generally similar among trees. One tree did not show increasing F_{d_out} in the growing season, since June 2011. As it was possible the tree was damaged by frequent sensor installation, we did not include it in the calculation of J_S and E_t. The daily J_S values calculated from Eq. (1) are shown in Figure 4a. Here, the values obtained from sample trees numbering four or more, and the values from a smaller number of trees than the minimum sample size are shown separately. Although the latter has lower representativeness, it is still worthwhile to include here in order to get a more complete view of seasonal J_s patterns.

The effect of annual defoliation on J_S was apparent in late January 2011 (Figure 4a). The abrupt decrease in F_d was observed in all of the five sample trees, which were measured in the leaf-fall period in 2011, including the trees in Group B. However, the trend was not clear in 2010. The result is consistent with observations that leaves at the lower canopy positions did not drop until May or June 2010. Even at the time of defoliation in 2011, J_S did not drop close to zero. While defoliation was observed to be more complete, some leaves remained on the trees until shortly after leaf flush. In addition, there is the possibility of increased measurement errors due to low sap velocity and contamination of the natural temperature gradient during the leaf-off period, as explained in the Sap flux measurements section. After leaf development in the late dry season (February–April), J_S increased gradually from the middle of March in 2010 after a few significant pre-monsoon rain events (see Figure 3b). Unfortunately, in 2011, the precise timing of the rise in J_S is not known due to the lack of data in May. In the early rainy season (May–July), J_S reached a maximum level; peaks appeared around the end of June and the magnitude was comparable in both years. In 2010, a decreasing trend in J_S was observed in the subsequent late rainy season (August–October). The J_S values dropped quickly to levels seen in the previous late dry season and these low rates continued through the early dry season (November–January). In contrast, in 2011, the J_S values experienced a sharp, but temporary depression in late September–early October before recovering and subsequently maintaining early dry season values at a higher level

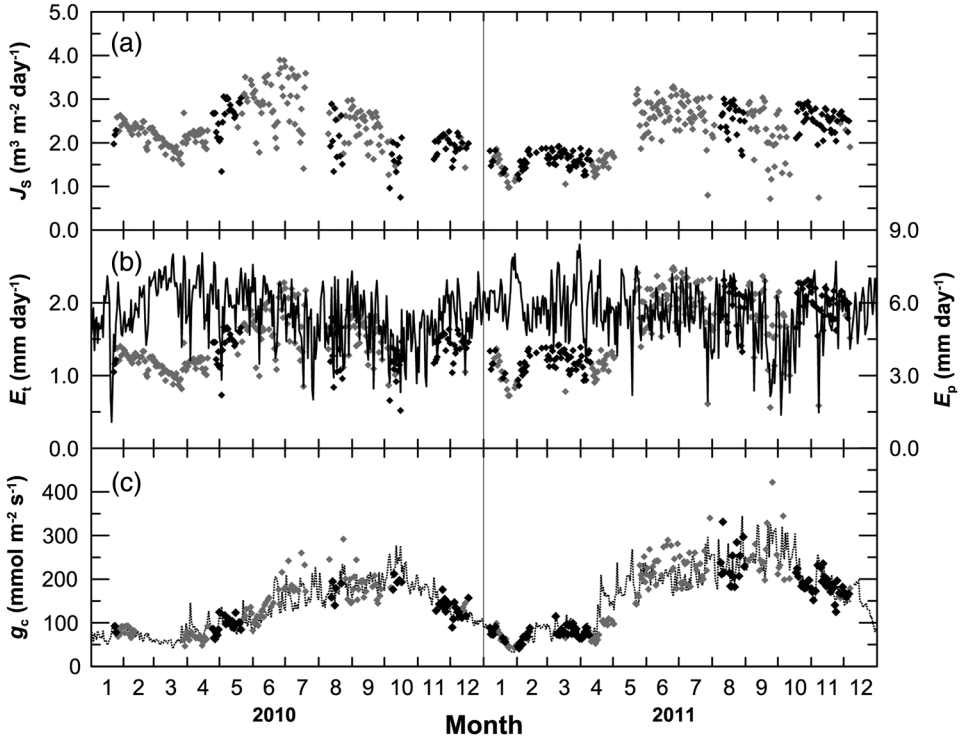

Figure 4. Seasonal patterns of (a) mean stand sap flux density (J_S), (b) stand transpiration rate (E_t) and potential evapotranspiration (E_p) and (c) canopy conductance (g_c). Data were integrated over one full day for J_S, E_t, while g_c was calculated as a daytime mean. Black symbols indicate the values from sample trees numbering four or more, while gray symbols indicate the values derived from a smaller number of trees. The dotted line in (b) represents E_p calculated from meteorological conditions using Eq. (13), and that in (c) represents g_c estimated by the best-fit model, which was determined by the non-linear multiple regression analysis.

than in 2010. The prolonged transpiration would be attributable to sunny conditions and a slow drop-off from the maximum leaf area probably caused by infrequent, but strong rain events (see Figure 3a and b).

Daily stand E_t values showed seasonal variation similar to that of the daily J_S (Figure 4b); however, they were not parallel because E_t increased due to an increase in sapwood area A_S that was associated with tree growth (see Eq. (2)). Although the magnitude of the J_S peak in 2011 was approximately the same as that in 2010, tree growth resulted in higher E_t through the year. The maximum daily stand E_t was ~2.0 mm day^{-1} in 2010 and ~2.4 mm day^{-1} in 2011. The potential evapotranspiration rate E_p had a similar seasonal pattern to D because of the relatively small variation in radiation throughout the year (see Figures 3b and d, 4b). The pattern of E_t was in good agreement with that of E_p throughout most of the rainy season (June–October), i.e., the ratio of E_t to E_p was nearly constant during that time. In the dry season, the E_t declined while the E_p increased, indicating very stressful conditions for trees.

Canopy conductance

To clarify environmental controls on transpiration of rubber trees, daytime mean canopy conductance g_c was calculated from Eq. (3) (Figure 4c). An annual cycle of g_c was apparent, with a maximum in September–October. The maximal value was higher in 2011 than in 2010 (300 versus 220 mmol m^{-2} s^{-1}). The g_c values, including only those obtained from sample trees numbering four or more, were compared with daytime averages of environmental factors and biometric parameters, such as downward shortwave radiation S_d, vapor pressure deficit D, relative extractable water in the soil Θ, air temperature T_a, leaf area index L_c, and sapwood area factor c_r. There was an exponential decrease in g_c with increasing D, and a logarithmic increase in g_c with increasing Θ (Figure 5b and c). A large part of the observed variability in these relationships resulted from year-to-year changes related to growth of the stand; g_c values demonstrated an upward shift during 2010 and 2011, especially in the rainy season. The g_c values also showed a linear relationship with increasing L_c and c_r (Figure 5e and f). Finally, while relationships between g_c and S_d and T_a were weak in light of dissimilarity between expected relationships (Eq. (6) and (9)) and upper boundaries of the data, the results suggest optimal conditions for the stomatal aperture of S_d of ~450 W m^{-2} and T_a of ~28 °C (Figure 5a and d). The results from the univariate analysis suggest that the stomatal apertures of rubber trees were strongly affected by atmospheric drought and soil moisture deficit as well as biometric parameters.

To examine the importance of each variable on g_c, non-linear multiple regression models were developed with different combinations of response functions, $f_1(S_d)$, $f_2(D)$, $f_3(\Theta)$, $f_4(T_a)$, $f_5(L_c)$, and $f_6(c_r)$, which are included in Eq. (5). Table 2 shows the resulting model parameters with standard errors and Akaike information criterion (AIC) values, which are used for model selection (e.g., Ford et al. 2005). Kumagai et al. (2008) showed that a combination of $f_1(S_d)$ and $f_2(D)$ is capable of predicting g_c values for Japanese cedar in the case of no limitation of soil moisture. However, when considering only these variables in the model, model parameters were not able to be determined due to a rank-deficient least-squares problem. To prevent such divergence, the response functions were included in decreasing order of strength of relationship between each variable and g_c as explained above. A second trial with $f_2(D)$ and $f_3(\Theta)$ resulted in parameters within an appropriate range, suggesting that soil moisture Θ was an essential factor to consider in the model. By adding $f_5(L_c)$ and $f_6(c_r)$ to the model, we obtained a drastic

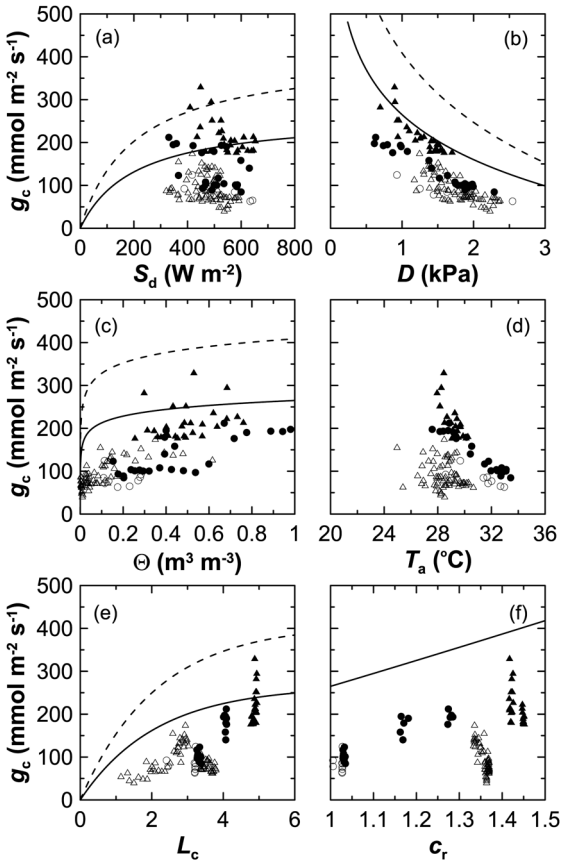

Figure 5. Relationships between canopy conductance (g_c) and (a) downward shortwave radiation (S_d), (b) vapor pressure deficit (D), (c) relative extractable water in the 0–0.5-m soil layer (Θ), (d) air temperature (T_a), (e) canopy leaf area index (L_c) and (f) sapwood area factor relative to the value on 1 January 2010 (c_r). Atmospheric conditions were measured above the canopy at 30-m height on the tower. Data were averaged over daytime values and shown separately with seasons: dry season of 2010 (January–April, open circles), rainy season of 2010 (May–October, closed circles), dry season of 2011 (November 2010–April, open triangles) and rainy season of 2011 (May–October, closed triangles). The lines represent modeled g_c constrained by the independent variable shown in each graph, and calculated by multiplying g_{cref} and the response function for each variable in the best-fit model; predictions are for 1 January 2010 (solid) and 31 December 2011 (dotted). The solid line in (f) denotes the fitted model equation for g_{cref}.

decrease in AIC. Consideration of $f_1(S_d)$ produced a small improvement in model performance. The final model with all functions, including $f_4(T_a)$, did not show improvements, although it resulted in a reasonable T_{opt} value of 26.4 °C. These results suggest that temperature, which remains at a high level throughout the whole year at the study site, was of minor importance in controlling the stomatal aperture of rubber trees.

The best prediction of g_c was obtained using the model with $f_1(S_d)$, $f_2(D)$, $f_3(\Theta)$, $f_5(L_c)$ and $f_6(c_r)$ (hereafter referred to as 'the best-fit model'). Modeled g_c values were consistent with measured values ($R^2 = 0.92$, $n = 157$) and the residual mean was zero (paired t-test; $P = 0.90$). The possibility of multicollinearity among the explanatory variables was rejected by confirming that variance inflation factors were sufficiently <10. Calculation of AICc, i.e., AIC with a correction for finite sample sizes, did not change the conclusion. Model performance was confirmed by the fact that most g_c observations were located between the best-fit curve and the x-axis when plotted versus the individual predictor variables (Figure 5). The same analysis was made with the same combination of response functions for individual years (Table 2); the results will be discussed below in the Inter-annual change in g_c sensitivity section.

Controls on annual transpiration rate

The best-fit model derived in the previous section was used to estimate the g_c values for 2010 and 2011 using an almost continuous record of meteorological data (see Figure 4c). These estimates were used to fill in missing values of sap-flow-derived g_c. The resulting dataset was then used to calculate E_t with Eq. (3). Since turbulence data, friction velocity u_* and sensible heat flux H, were frequently missing due to sensor wetting by rainfall, aerodynamic conductance g_a and canopy surface temperature T_s should be estimated in other ways. The g_a values were estimated from the observed linear relationship between daytime mean g_a and wind speed U above the canopy ($g_a = 1.042U + 2.597$, $R^2 = 0.78$, $n = 367$). Radiometric surface temperature, which was calculated from observed upward longwave radiation by assuming a surface emissivity of 0.987 for green broadleaf forest (Snyder et al. 1998), was substituted for T_s. Three days of missing data for precipitation rate P_r and E_t in 2011 were assumed to be negligible in the annual estimation. The estimated annual E_t was 469 mm year^{-1} in 2010 and 658 mm year^{-1} in 2011. The increasing trend in the annual E_t was consistent with that in annual P_r. The annual rate of increase (R_I) was 40.3% for E_t and 16% for P_r, resulting in an increased ratio of E_t to P_r from 35.2 to 42.6%.

The increase in E_t in 2011 over the previous year implies either less stress from atmospheric and soil drought on the rubber trees, or an effect of increased tree size (L_c and d). To judge which effect was more important, diagnostic analyses were performed using Eq. (3) and the best-fit model of g_c with changing constituent variables (Table 3). First, non-limiting water in the soil, $\Theta = 1$, was assumed throughout the year with the other variables assigned their observation values. The calculated hypothetical E_t was 12–17% larger than the observed E_t, indicating that soil water deficit would have limited tree transpiration. This change, however, did not close the E_t gap

Table 3. Annual transpiration rate (E_t) in mm year^{-1} in the rubber stand during 2010 and 2011 estimated using Eq. (3) with the best-fit model of canopy conductance. For each E_t calculation, variables in parentheses were assumed to be constant throughout the year, with the other variables assigned their observed values.

	2010	2011	R_I (%)[2]
E_t[1]	469	658	40.3
$E_t(\Theta = 1)$	523	770	47.2
$E_t(D = 1$ kPa)	459	645	40.5
$E_t(L_c = 3)$	452	613	35.6
$E_t(c_r = 1)$	408	460	12.7
$E_t(L_c = 3, c_r = 1)$	395	428	8.4

[1]Calculation based on observed data.
[2]R_I indicates the annual rate of increase in E_t of 2011 over the previous year.

Table 2. Model parameters (±standard error) and AIC obtained by the non-linear multiple regression analysis of Eq. (5) for possible predictor combinations. The model parameters g_{cref0} (mmol m^{-2} s^{-1}), α, β_1, β_2, β_3, β_4, T_{opt} (°C) are given in Eq. (6–12). Parameters are also shown for 2010 and 2011 separately after determining the best predictor combination and using fixed values of g_{cref0} and β_4 determined from both years of data.

Predictors[1]	g_{cref0}	α	β_1	β_2	β_3	β_4	T_{opt}	AIC
S_d, D	–	–	–					–
D, Θ	226.0 ± 5.4		0.60 ± 0.04	0.25 ± 0.02				360.8
D, Θ, L_c	934.6 ± 527.6		0.46 ± 0.04	0.18 ± 0.02	0.06 ± 0.04			249.0
D, Θ, L_c, c_r	196.9 ± 18.7		0.46 ± 0.03	0.22 ± 0.02	0.38 ± 0.06	1.14 ± 0.13		189.7
S_d, D, Θ, L_c, c_r	265.0 ± 34.9	203 ± 81	0.57 ± 0.04	0.20 ± 0.02	0.47 ± 0.08	1.12 ± 0.13		178.7
S_d, D, Θ, T_a, L_c, c_r	300.1 ± 58.8	194 ± 81	0.53 ± 0.05	0.20 ± 0.02	0.40 ± 0.09	0.91 ± 0.21	26.4 ± 2.2	185.2
								year
S_d, D, Θ, L_c, c_r	265.0[2]	18 ± 62	0.39 ± 0.07	0.00 ± 0.07	0.20 ± 0.04	1.12[2]		2010
S_d, D, Θ, L_c, c_r	265.0[2]	188 ± 35	0.66 ± 0.03	0.19 ± 0.02	0.49 ± 0.11	1.12[2]		2011

[1]S_d, downward shortwave radiation; D, vapor pressure deficit; Θ, relative extractable water in the 0–0.5 m soil layer; L_c, leaf area index; c_r, factor of sapwood area relative to the value on 1 January 2010; T_a, air temperature.
[2]These values are fixed in the regression analysis.

between the 2 years in light of increased R_l. Given continuous non-drought atmospheric conditions, $D = 1$ kPa, hypothetical E_t values were almost the same as observations, and R_l did not change. Environmental conditions such as soil water deficit or atmospheric drought, therefore, did not account for the large R_l. An assumption of constant L_c brought an R_l decrease of 4.7%. In contrast, neglecting tree growth, by making c_r constant, decreased R_l substantially. The observed R_l of 40.3% was mostly explained by the changes in L_c and d. Together they accounted for 80% of the E_t difference, suggesting that inter-annual change of E_t was determined primarily by tree growth rate, not by environmental changes in the air and the soil. Again the study rubber stand was characterized by rapid growth, especially during the rainy season in 2010.

Discussion

Tree maturity and latex tapping

The study rubber trees were 7–8 years old and mature in a reproductive sense. Unlike immature rubber trees, mature trees exhibit annual shedding of senescent leaves (Priyadarshan 2011), affecting the observed annual pattern of leaf area index L_c with increasing stand age. The defoliation, referred to as 'wintering', is usually seen in rubber trees of >4 years, and transition to the reproductive stage coincides with it (Priyadarshan 2011). In the two study years, however, the difference in the manner of defoliation was observed as mentioned in the sections Meteorological conditions and stand biometric parameters and Transpiration rate at individual tree and stand scale. The trees in January 2010 did not drop all of their leaves, but in January 2011 they did drop nearly all of their leaves. Presumably, the greater 2011 defoliation was caused by drier conditions at the start of the year in 2011 than 2010 (see Figure 3e). Previous studies on water relations of rubber trees have found a large difference in L_c between rainfed and irrigated plots in the dry season (Vijayakumar et al. 1998, Devakumar et al. 1999), suggesting a relationship between soil moisture and the degree of dry season defoliation.

Generally, the term of maturity is used in the reproductive sense, but many studies have confounded tree size increase with the stage transition (Bond 2000). The same is true for rubber trees; some studies have used the term 'mature' for trees that have reached a size appropriate for latex extraction (Chandrashekar et al. 1998, Gunasekara et al. 2007). Latex tapping in this plantation is generally withheld for 6 years after planting of nursery trees, or until a certain percentage of trees reach 0.5 m of girth. The year 2010 coincided with the final year of non-tapping treatment; tapping was commenced in November of that year. In this sense, the study rubber trees reached a mature state at the end of 2010. A drastic change occurred in tree size development; a large decline in stem growth rate was observed in 2011 when compared with 2010. This is thought to be largely the result of latex tapping, started in November 2010, which acts as a competing carbohydrate sink. Our observation was consistent with the previous finding that radial growth of rubber begins with the onset of the rainy season and lasts until the onset of the dry season in untapped control trees, and the growth rate is drastically reduced in tapped trees (Silpi et al. 2006).

Transpiration under severe drought conditions

Observed J_S, E_t, and g_c remained above zero under severe drought conditions despite extractable surface-layer soil moisture being nearly depleted in the period from the beginning of February to the middle of April of 2011 (see Figures 3e and 4). The minimum value of relative extractable water in the soil Θ depends on the residual water content θ_r. We did not determine θ_r experimentally and, instead, assigned to this parameter the minimum value of soil water content observed during the two study years (Meteorological measurements section). According to Genuchten (1980), θ_r is defined as the water content at a soil suction of 1500 kPa, i.e., at the permanent wilting point of plants. In fact, however, rubber trees were apparently not seriously damaged by the prolonged drought at near the minimum soil water content, and, rather, continued to transpire at a low level. Although it is plausible that actual θ_r was lower than the assigned value, the fact that Θ did not change much during this period suggests that little or no water was being extracted from the 0–0.5-m layer. Thus, it is more likely that rubber trees could tap deeper soil water to maintain a low level of transpiration even when the upper soil layer was severely desiccated.

In the study rubber stand, it was observed that tap roots reached at least 3-m depth. It was also observed that fine roots were highly concentrated in the top 0–0.2-m soil, and below 0.5 m roots became much more sparse. These facts are consistent with previous knowledge that rubber tree roots can extend in depth >4 m below the surface, but the majority of roots are found within 0.3 m of the soil surface (Carr 2012). In a mature rubber plantation in southern India, George et al. (2009) found that root water uptake was highest in the top 0.1-m soil and declined substantially at 0.9-m depth. In Thailand, however, Gonkhamdee et al. (2009) observed root growth in the soil deeper than 1.5 m in the dry season. Analyzing soil water balance in a rubber plantation in Xishuangbanna, Guardiola-Claramonte et al. (2008) found an increase in root water uptake from the deeper layers starting in the middle of the dry season, while soil moisture remained constant in the surface layer. In the study rubber stand, the same phenomenon was inferred from the soil moisture measurements in the deep-soil layer (1–3.4 m) in the dry season of 2011 (data not shown). In the driest period, during the week before a small pre-monsoon rain event on 8 May, constant soil moisture was observed over the entire soil layer. Thus, the observed non-zero transpiration rates were at least partly attributable to water uptake from the soil layer below 0.5 m, and in an extreme case, only attributable to that below 3.4 m.

Potential transpiration rate

To examine the potential of rubber trees to transpire, the value of g_{cref} in the best-fit model (see Table 2) was compared with the values summarized for several different tree species by Oren et al. (1999). For the comparison, g_{cref} was converted to a reference value of canopy stomatal conductance (g_{sref}) by dividing by critical L_c (hereafter referred to as L_{c*}), which is the value of L_c at which g_c values were minimally constrained by leaf area. In other words, the L_{c*} corresponds to the L_c at which $f_5(L_c)$ gives the value closest to unity. In the present study, L_{c*} was set to the maximum observed value of L_c, 5.0, at which $f_5(L_c) = 0.91$ (see Figure 5e). The g_{sref} values summarized by Oren et al. (1999) were obtained from g_c on an hourly or half-hourly basis. Our values were determined on a daytime mean basis. As expected from the diurnal course, daytime mean values have a smaller maximal value compared with hourly mean values, and thus our g_{cref} and g_{sref} would not be comparable. Based on the ratio of half-hourly mean E_t around noon to daytime mean E_t of ~1.17, g_{cref} and g_{sref} corresponding to half-hourly near-noon data would be 310 and 62 mmol m^{-2} s^{-1}, respectively, for 1 January 2010. Because g_{cref} is represented by a function of c_r (see Eq. (11)), these values would increase to 474 and 95 mmol m^{-2} s^{-1}, respectively, for 31 December 2011. Oren et al. (1999), compiling the g_{sref} values of diffuse-porous species from prior studies, reported an average of 93 mmol m^{-2} s^{-1}. Our g_{sref} value was relatively low at the beginning of the study, but it was comparable to the average reported by Oren et al. (1999) by the end of the study period due to the rapid stem growth of the rubber trees. Given that the trees continue to grow and an increase in maximum L_c is likely, the 7–8-year-old rubber trees studied here would be expected to rank high among diffuse-porous species within a few years time.

Sensitivity of stomatal regulation to atmospheric drought

The sensitivity of stomatal regulation to atmospheric drought is represented by β_1, which corresponds to m/b, where b represents g_{cref} and m the sensitivity of g_c to vapor pressure deficit D (i.e., intercept and slope of a linear regression between g_c and $-\ln D$). Explanation is provided by Oren et al. (1999), who showed experimentally and theoretically that this parameter should be 0.6 for plants with perfect stomatal regulation of a minimum leaf water potential with respect to D. The value from our best-fit model was 0.57 ± 0.04 (Table 2), and the 95% CI was 0.50–0.65. The results indicate that the study rubber trees demonstrate stomatal sensitivity to the atmospheric drought. As suggested by Rao et al. (1990), the clonal difference in terms of water relations is large in rubber trees. Nevertheless, the same conclusion was drawn by Isarangkool Na Ayutthaya et al. (2011), who observed isohydric behavior in a different clone (RRIM 600), measuring nearly constant midday leaf water potential under different conditions of atmospheric evaporative demand as well as soil drought. In contrast, Sangsing et al. (2004) found anisohydric behavior in young RRIM 600 trees. The possibility of change in stomatal regulation associated with tree growth will be discussed later.

Sensitivity of g_c to the other variables

The parameters of α, β_2, β_3, and β_4 represent g_c sensitivities to downward shortwave radiation S_d, Θ, L_c, and sapwood area factor c_r. The best-fit model produced an α value of 203, which was >82 for a 35-year-old sessile oak (*Quercus petraea* (Matt.) Liebl.) stand (Granier and Bréda 1996) or 78–135 for a Japanese cedar stand (Kumagai et al. 2008). Larger α indicates that g_c has fewer incidences of light saturation. However, the 95% CI was very wide, 44–363, indicating the futility of investigating this parameter further. Dependency of g_c on S_d was not well constrained, probably due to a small range of daily mean S_d observed over the study rubber stand (300–650 W m^{-2}) as shown in Figure 5a. As mentioned in Canopy conductance section, incorporation of $f_1(S_d)$ contributed to an improvement in g_c model performance, but not significantly, in light of a small decrease in AIC value with the addition of $f_1(S_d)$ (Table 2). Therefore, the uncertainty in α determination would not have much effect on the model.

Several studies have investigated β_2. Granier and Bréda (1996) derived a β_2 value of 0.56 for a 35-year-old sessile oak stand, and Pataki and Oren (2003) obtained 0.45 for tulip (*Liriodendron tulipifera* L.) trees. The β_2 value obtained in our rubber stand, 0.20 (95% CI 0.16–0.23), was lower than the values from previous studies. Smaller β_2 indicates that g_c is less sensitive to the change in soil water availability. Despite the fact that non-linear regression analysis suggests a strong dependence of g_c of rubber trees on Θ, the g_c was predicted to remain at a high level until soil moisture reached very low values (Figure 5c). The result is consistent with the study on other rubber trees by Isarangkool Na Ayutthaya et al. (2011), who observed that whole-tree hydraulic conductance (K_T) remained constant at its maximum value over a wide range of Θ, except at the lower end. Although the behavior of K_T does not necessarily correspond to that of g_c, a strong linear relationship between them has been observed in many species (e.g., Meinzer and Grantz 1990, Hubbard et al. 2001), probably because stomatal control of leaf gas exchange is coupled to the plant hydraulic system (Franks 2004). Therefore, rubber trees might be vulnerable to drought because they do not minimize water use as soil moisture declines, allowing soil water reserves to be nearly depleted before reducing g_c. The magnitude of β_2 and implications regarding rubber tree drought vulnerability were unchanged if the Θ was estimated from soil moisture content measured for the 0–3.4-m layer (data not shown).

The β_3 value of 0.47 (95% CI 0.32–0.62) indicates that g_c would not increase further with L_c >6 (Figure 5e) due to the effect of light competition between the upper and lower leaves

in the canopy. This finding is consistent with previous studies (e.g., Kelliher et al. 1995, Granier et al. 2000), suggesting that the estimated seasonal pattern of L_c, which was based on a limited number of observations (see Stem diameter and leaf area index section), is reasonable. The β_4 value of 1.12 can be regarded as nearly unity in light of the 95% CI range 0.87–1.38. As mentioned in the Calculation of canopy conductance section, increasing c_r changes E_t, and thus g_c. The effect of partial decoupling between the canopy and the atmosphere and the effect of increased root development would result in β_4 larger than unity, while the effect of increased xylem resistance would act in the opposite direction. The derived β_4 close to unity suggests that these positive and negative effects on g_c were nearly balanced or were each negligible in the rubber stand.

Inter-annual change in g_c sensitivity

To examine the effects of tree maturity and the initiation of latex tapping on g_c, data in 2010 and 2011 were separately fit to Eq. (5) with the same combination of response functions in the best-fit model for the 2 years (Table 2). In this analysis, g_{cref0} and β_4 values were fixed at 265 mmol m^{-2} s^{-1} and 1.12, respectively, from the analysis for the 2 years, as they could not be determined robustly without a wide range of stem diameter d. Modeled g_c values again explained observed values well in each year (2010: $R^2 = 0.86$, $n = 54$; 2011: $R^2 = 0.95$, $n = 103$). The analysis suggests that g_c sensitivity to the constituent variables, S_d, D, Θ and L_c, derived from 2 years of data reflected the g_c behavior in 2011. The parameters obtained for 2010 indicate lower sensitivity to all of the variables. In particular, α and β_2 values were not significantly different from zero at the 95% level of confidence. The results indicate that stomatal regulation of younger and non-tapped rubber trees is less sensitive to air and soil environmental variables. However, although it is difficult to differentiate the effects of tree maturity versus latex tapping on g_c, stomatal regulation of mature rubber trees undergoing tapping is more sensitive. The studied clone RRIC 100 belongs to the high growth and drought-tolerant group based on experiments in young rubber trees (Chandrashekar et al. 1998). It is conceivable that young rubber trees can achieve high carbon gain by exhibiting anisohydric behavior (Kumagai and Porporato 2012) despite having restricted g_{cref} due to immature leaves and small conductive xylem area. It can also be inferred that carbon extraction by latex tapping forces rubber trees to be more thrifty with water. Two years of data are insufficient to make firm conclusions about the effects of tree maturity or latex tapping on g_c, and further study is warranted to understand rubber tree physiology in different development stages.

Sensitivity of E_t to atmospheric variability

The difference in evaporative demand between the 2 years was relatively small based on the potential evapotranspiration rate E_p calculated from Eq. (13). The estimated annual E_p was 2013 mm $year^{-1}$ in 2010, and 2041 mm $year^{-1}$ in 2011. There is little information about the range of variability in the relevant meteorological conditions in central Cambodia, especially D and net radiation R_n, which are primary determinants of E_p. However, observations at a meteorological station in Phnom Penh, ~83 km southwest of our study site, are available from 'Global Summary of the Day' distributed by the National Climatic Data Center (NCDC 2012). Based on data over 10 years (2003–2012), annual mean D had a σ of 0.30 kPa with a range of 0.84–1.69 kPa. By comparing dry and rainy seasons, Tsujimoto et al. (2008) have suggested that the effects of variations in cloud cover on R_n are muted in this region, because rainfall events tend to occur during evening and night, and because of the compensating increase in downward longwave radiation by clouds. Indeed, annual R_n at the study site in 2011 increased over the previous year, but by only 2.2%, despite a 15.8% increase in precipitation rate P_r. Actual E_t is affected by soil water availability as well as the evaporative demand. The soil water availability is strongly related to P_r. As mentioned in the Site description section, we have long-term P_r data over 10 years (2000–2009) in the study rubber plantation. Annual values showed a remarkably wide range, 986–1678 mm. These observational results suggest that conditions during our two experimental years are normal, and dryer or wetter conditions can occur at short intervals.

To investigate effects of the possible variability in D and P_r on annual E_t, we repeated the analysis described in the Controls on annual transpiration rate section, but for hypothetical cases of higher D and both higher and lower Θ. We began by setting D 1.5 times larger than observed, keeping the other variables as observed. Because annual mean D observed was ~1 kPa in both years, the hypothetical analysis was conducted for a possible dry year with annual mean D ~1.5 kPa. The resulting hypothetical E_t values were 469 mm $year^{-1}$ in 2010 and 663 mm $year^{-1}$ in 2011, negligibly different from the observed E_t in both years (see Table 3). The small increase under higher evaporative conditions can be explained by the compensating effect of higher D on g_c, i.e., decreased stomatal aperture in response to drought stress. Next, soil moisture was set to observed Θ to the 2nd power and to the 1/2 power to represent conditions dryer and wetter than average, respectively. Predicted E_t values were 411 mm $year^{-1}$ in 2010 and 542 mm $year^{-1}$ in 2011 for dryer conditions, and 495 mm $year^{-1}$ in 2010 and 714 mm $year^{-1}$ in 2011 for wetter conditions. Changes from the observed annual E_t values ranged from –116 to 56 mm $year^{-1}$. The resulting change in E_t was smaller than the observed difference in E_t, 189 mm between the 2 years.

The large effect of tree growth compared with environmental changes on annual E_t of young rubber trees was suggested based on the 2 years of data presented here (see Controls on annual transpiration rate section). We conclude that, at this stage of growth (7–8 years old), the effect of rapid tree growth

on E_t would have overwhelmed the effect of environmental changes, even if the changes had been extreme. Some previous studies have reached the same conclusion that A_S is a major determinant of water use in forest stands (Dunn and Connor 1993, Ewers et al. 1999, Kumagai et al. 2007, 2008). Even in a stand with large horizontal moisture gradients in the soil, it has been observed that whole-tree J_s did not show systematic variation in space, but E_t did vary spatially because of differences in the A_S of individual trees (Adelman et al. 2008, Loranty et al. 2008).

Transpiration rate of rubber with that of other tropical trees

For the study rubber plantation, the maximum rainy-season values of E_t were ~2.0–2.4 mm day^{-1}, comparable to the ~2.0 mm day^{-1} observed for another rubber clone in northeast Thailand (Isarangkool Na Ayutthaya et al. 2011), but smaller than ~3.5 and 4.5 mm day^{-1} for two rubber clones in southern India (Rao et al. 1990). Perhaps because of the difficulty in measuring sap flow of numerous species in diverse stands and scaling up from the individual tree to the stand level, very few studies have been carried out on natural tropical forest transpiration against which we could compare the results for rubber transpiration. The few studies available include one for a mixed dipterocarp forest in Borneo island, where Becker (1996) reported a mean wet season E_t, based on sap flux measurements, of ~1.3 mm day^{-1}, ~40% lower than the E_t for the study rubber plantation. In contrast, Kumagai et al. (2004), also for a mixed dipterocarp forest in Borneo, estimated an E_t of 3.5 mm day^{-1}, ~60% higher than rubber E_t, based on eddy covariance measurements with assumption of negligible soil surface evaporation under the dense canopy. The rubber E_t was not remarkably high compared with other major plantation trees in the same tropical region, including ~2.3 and 3.9 mm day^{-1} for acacia (*Acacia mangium* Willd.) plantations in Borneo (Cienciala et al. 2000), ~5.7 and 5.0 mm day^{-1} for eucalyptus (*Eucalyptus tereticornis* Sm.) plantations in southern India (Kallarackal and Somen 1997) and ~3.6 mm day^{-1} for a teak (*Tectonagrandis* L. f.) plantation in northern Thailand (Tanaka et al. 2009). The comparison above suggests that there is no conclusive evidence that rubber trees have the traits of a high water consumer.

Conclusions

Intra- and inter-annual variations in the transpiration rate, E_t, of rubber trees growing in central Cambodia were examined over 2 years. Observed xylem sap flux density, F_d, showed similar seasonal patterns among individual trees, probably because they were of the same clone and same age. Mean stand sap flux density, J_S, indicates rubber trees actively transpire in the rainy season, but become less active in the dry season. In the second study year, rubber trees shed their leaves almost completely in late January, and J_S dropped dramatically in synchronization with the shedding. Although J_S was restored soon after new leaf development, J_S increased significantly at the onset of the rainy season. Maximal values of E_t were observed in the middle of the rainy season, reaching ~2.0 mm day^{-1} in 2010 and ~2.4 mm day^{-1} in 2011.

To clarify environmental controls on rubber transpiration, canopy conductance, g_c, was calculated on a daytime basis. A non-linear multiple regression analysis was conducted for the 2 years of data, and a best-fit model was determined in light of the lowest AIC. Observed g_c values were well explained by the changes in S_d, D, Θ, L_c, and c_r. Factors of D, Θ, L_c, and c_r were of major importance, while S_d was of minor importance. Compared with the average value of diffuse-porous species from previous studies (Oren et al. 1999), the reference value of canopy stomatal conductance, g_{sref}, was relatively small in the beginning of the study period, but it was comparable to other species after 2 years due to rapid stem growth. The β_1 sensitivity parameter to D was very close to the value of 0.6, suggesting isohydric behavior of rubber trees (Oren et al. 1999). The β_2 sensitivity parameter to Θ suggests relatively low sensitivity of rubber g_c to soil water deficit except under extreme drought conditions. The same analysis for each year suggests that stomatal regulation of younger untapped rubber trees tends to be less sensitive to atmospheric and soil moisture conditions than more mature tapped trees.

The best-fit model was utilized to interpolate g_c values through the 2 years, and the continuous g_c and meteorological data were used to estimate annual E_t. Estimated E_t was 469 mm year^{-1} in 2010 and 658 mm year^{-1} in 2011. To determine the reason for the observed 40.3% increase in annual E_t in 2011 compared with the previous year, a diagnostic analysis was conducted by changing constituent variables in the calculation. As a result, the most important factor was c_r followed by L_c. Factors related to tree growth explained 80% of the annual increase in E_t, while changes in environmental conditions (in the air and soil) had minor effects. In particular in the early stage of rubber tree development when rubber growth is rapid, frequent measurements of tree size would be crucial to predict the level of water consumption. To extend our results to a regional scale, future research should focus on the potentially broad applicability of the relationship between E_t and tree size as well as environmental factors in stands different in terms of clonal type and age.

Our finding suggests moderate E_t for rubber compared with other tropical plantations. However, the strong positive relationship between g_c and sapwood area implies a potential for rubber trees to be a high water consumer in a more mature state. Because an increase in tree basal area does not necessarily mean a proportional increase in sapwood area in the presence of formation of less conductive area near the pith as observed by Isarangkool Na Ayutthaya et al. (2010), it is crucial

to further investigate the change in radial variation of xylem hydraulic conductivity with growth. In the study plot, the percentage of trees that died before reaching maturity was relatively higher than neighboring plots, which may have caused us to underestimate stand E_t to some extent. Although concerns raised by Guardia-Claramonte et al. (2008) and Tan et al. (2011), i.e., depletion in deep-soil moisture or steam desiccation due to large water uptake by rubber trees, would be partly explained by the low ability of rubber trees to conserve the soil water found in the present study, high evapotranspiration could also be attributable to other water loss components, e.g., wet-canopy evaporation, soil evaporation and transpiration of understory vegetation. To obtain a clear picture of the water budget of a rubber plantation and predict the sustainability of rubber cultivation with regard to its water use, we need to further investigate processes at different scales, i.e., canopy, trees, and leaves, in a comprehensive manner.

Acknowledgments

The study rubber plantation is managed by the Cambodian Rubber Research Institute (CRRI). We are grateful to the staff of CRRI for their help in the field experiments. We also thank Dr Nobuya Mizoue and Mr Khun Kakada of Kyushu University for their support, and our colleagues in the Eco-Climate System Laboratory, Hydrospheric Atmospheric Research Center (HyARC) of Nagoya University for their helpful comments.

Conflict of interest

None declared.

Funding

This study was conducted primarily under the projects 'Estimation and simulation of carbon stock change of tropical forest in Asia (2011–2014)' funded by the Ministry of Agriculture, Forestry and Fisheries, Japan. Also, this study was supported in part by a Grant-in-Aid for Scientific Research (23405028) and the granted project 'Program for risk information on climate change' from the Ministry of Education, Science and Culture, Japan. Participation of R.G.M., T.W.G. and A.D.Z. was supported by NASA grants NNG04GH59G and NNX08AL90G.

References

Adelman J, Ewers B, MacKay D (2008) Use of temporal patterns in vapor pressure deficit to explain spatial autocorrelation dynamics in tree transpiration. Tree Physiol 28:647–658.

Becker P (1996) Sap flow in Bornean heath and dipterocarp forest trees during wet and dry periods. Tree Physiol 16:295–299.

Bond BJ (2000) Age-related changes in photosynthesis of woody plants. Trends Plant Sci 5:349–353.

Brutsaert W (ed) (1982) Evaporation into the atmosphere. Reidel, Dordrecht.

Brutsaert W (1999) Aspects of bulk atmospheric boundary layer similarity under free-convective conditions. Rev Geophys 37:439–451.

Carr MKV (2012) The water relations of rubber (*Hevea brasiliensis*): a review. Exp Agric 48:176–193.

Čermák J, Kučera J, Nadezhdina N (2004) Sap flow measurements with some thermodynamic methods, flow integration within trees and scaling up from sample trees to entire forest stands. Trees Struct Funct 18:529–546.

Chandrashekar TR, Nazeer MA, Marattukalam JG, Prakash GP, Annamalainathan K, Thomas J (1998) An analysis of growth and drought tolerance in rubber during the immature phase in a dry subhumid climate. Exp Agric 34:287–300.

Cheng Y, Brutsaert W (2005) Flux-profile relationships for wind speed and temperature in the stable atmospheric boundary layer. Bound Layer Meteorol 114:519–538.

Cienciala E, Kučera J, Malmer A (2000) Tree sap flow and stand transpiration of two *Acacia mangium* plantations in Sabah, Borneo. J Hydrol 236:109–120.

Clearwater M, Meinzer F, Andrade J, Goldstein G, Holbrook N (1999) Potential errors in measurement of nonuniform sap flow using heat dissipation probes. Tree Physiol 19:681–687.

Devakumar AS, Gawai Prakash P, Sathik MBM, Jacob J (1999) Drought alters the canopy architecture and micro-climate of *Hevea brasiliensis* trees. Trees 13:161–167.

Dunn G, Connor D (1993) An analysis of sap flow in mountain ash (*Eucalyptus regnans*) forests of different age. Tree Physiol 13:321–336.

Ewers B, Oren R, Albaugh T, Dougherty P (1999) Carry-over effects of water and nutrient supply on water use of *Pinus taeda*. Ecol Appl 9:513–525.

FAO (2010) FAOSTAT. http://www.faostat.fao.org/ (8 November 2012, date last accessed).

Ford C, Goranson C, Mitchell R, Will R, Teskey R (2005) Modeling canopy transpiration using time series analysis: a case study illustrating the effect of soil moisture deficit on *Pinus taeda*. Agric For Meteorol 130:163–175.

Franks PJ (2004) Stomatal control and hydraulic conductance, with special reference to tall trees. Tree Physiol 24:865–878.

George S, Suresh PR, Wahid PA, Nair RB, Punnoose KI (2009) Active root distribution pattern of *Hevea brasiliensis* determined by radioassay of latex serum. Agrofor Syst 76:275–281.

Gonkhamdee S, Maeght JL, Do FC, Pierret A (2009) Growth dynamics of fine *Hevea brasiliensis* roots along a 4.5-m soil profile. Khon Kaen Agric J 37:265–276.

Granier A (1987) Evaluation of transpiration in a Douglas-fir stand by means of sap flow measurements. Tree Physiol 3:309–320.

Granier A, Bréda N (1996) Modelling canopy conductance and stand transpiration of an oak forest from sap flow measurements. Ann Sci For 53:537–546.

Granier A, Loustau D, Bréda N (2000) A generic model of forest canopy conductance dependent on climate, soil water availability and leaf area index. Ann For Sci 57:755–765.

Guardiola-Claramonte M, Troch PA, Ziegler AD, Giambelluca TW, Vogler JB, Nullet MA (2008) Local hydrologic effects of introducing non-native vegetation in a tropical catchment. Ecohydrol 1:13–22.

Guardiola-Claramonte M, Troch PA, Ziegler AD, Giambelluca TW, Durcik M, Vogler JB, Nullet MA (2010) Hydrologic effects of the expansion of rubber (*Hevea brasiliensis*) in a tropical catchment. Ecohydrol 3:306–314.

Gunasekara H, De Costa W, Nugawela E (2007) Genotypic variation in canopy photosynthesis, leaf gas exchange characteristics and their response to tapping in rubber (*Hevea brasiliensis*). Exp Agric 43:223–240.

Hubbard RM, Ryan MG, Stiller V, Sperry JS (2001) Stomatal conductance and photosynthesis vary linearly with plant hydraulic conductance in ponderosa pine. Plant Cell Environ 24:113–121.

Isarangkool Na Ayutthaya S, Do FC, Pannengpetch K, Junjittakarn J, Maeght JL, Rocheteau A, Cochard H (2010) Transient thermal dissipation method of xylem sap flow measurement: multi-species calibration and field evaluation. Tree Physiol 30:139–148.

Isarangkool Na Ayutthaya S, Do FC, Pannangpetch K, Junjittakarn J, Maeght JL, Rocheteau A, Cochard H (2011) Water loss regulation in mature *Hevea brasiliensis*: effects of intermittent drought in the rainy season and hydraulic regulation. Tree Physiol 31:751–762.

Jarvis PG (1976) The interpretation of the variations in leaf water potential and stomatal conductance found in canopies in the field. Philos Trans Royal Soc Lond B 273:593–610.

Jarvis PG, McNaughton KG (1986) Stomatal control of transpiration: scaling up from leaf to region. Adv Ecol Res 15:1–49.

Kaimal JC, Finnigan JJ (1994) Atmospheric boundary layer flows: their structure and management. Oxford University Press, New York, 289 p.

Kallarackal J, Somen CK (1997) Water use by *Eucalyptus tereticornis* stands of differing density in southern India. Tree Physiol 17:195–203.

Kelliher FM, Leuning R, Raupach MR, Schulze ED (1995) Maximum conductances for evaporation from global vegetation types. Agric For Meteorol 73:1–16.

Kobayashi N, Hiyama T, Fukushima Y, Lopez ML, Hirano T, Fujinuma Y (2007) Nighttime transpiration observed over a larch forest in Hokkaido, Japan. Water Resour Res 43:W03407.

Kumagai T, Porporato A (2012) Strategies of a Bornean tropical rainforest water use as a function of rainfall regime: isohydric or anisohydric? Plant Cell Environ 352:61–71.

Kumagai T, Saitoh TM, Sato Y, Morooka T, Manfroi OJ, Kuraji K, Suzuki M (2004) Transpiration, canopy conductance and the decoupling coefficient of a lowland mixed dipterocarp forest in Sarawak, Borneo: dry spell effects. J Hydrol 287:237–251.

Kumagai T, Aoki S, Nagasawa H, Mabuchi T, Kubota K, Inoue S, Utsumi Y, Otsuki K (2005) Effects of tree-to-tree and radial variations on sap flow estimates of transpiration in Japanese cedar. Agric For Meteorol 135:110–116.

Kumagai T, Aoki S, Shimizu T, Otsuki K (2007) Sap flow estimates of stand transpiration at two slope positions in a Japanese cedar forest watershed. Tree Physiol 27:161.

Kumagai T, Tateishi M, Shimizu T, Otsuki K (2008) Transpiration and canopy conductance at two slope positions in a Japanese cedar forest watershed. Agric For Meteorol 148:1444–1455.

Kumagai T, Mudd RG, Miyazawa Y et al. (2013) Simulation of canopy CO_2/H_2O fluxes for a rubber (*Hevea brasiliensis*) plantation in central Cambodia: The effect of the regular spacing of planted trees. Ecol Model 265:124–135.

Kume T, Tsuruta K, Komatsu H, Kumagai T, Higashi N, Shinohara Y, Otsuki K (2010) Effects of sample size on sap flux-based stand-scale transpiration estimates. Tree Physiol 30:129–138.

Li Z, Fox JM (2012) Mapping rubber tree growth in mainland Southeast Asia using time-series MODIS 250m NDVI and statistical data. Appl Geogr 32:420–432.

Loranty M, Mackay D, Ewers B, Adelman J, Kruger E (2008) Environmental drivers of spatial variation in whole-tree transpiration in an aspen-dominated upland-to-wetland forest gradient. Water Resour Res 44:W02441.

Meinzer FC, Grantz DA (1990) Stomatal and hydraulic conductance in growing sugarcane: stomatal adjustment to water transport capacity. Plant Cell Environ 13:383–388.

Mölder M, Lindroth A (2001) Dependence of kB^{-1} factor on roughness Reynolds number for barley and pasture. Agric For Meteorol 106: 147–152.

NCDC (2012) Global surface summary of the day, http://www.ncdc.noaa.gov/cgi-bin/res40.pl?page = gsod.html (11 January 2013, date last accessed).

Ohta T, Hiyama T, Tanaka H, Kuwada T, Maximov TC, Ohata T, Fukushima Y (2001) Seasonal variation in the energy and water exchanges above and below a larch forest in Eastern Siberia. Hydrol Process 15:1459–1476.

Oren R, Sperry JS, Katul GG, Pataki DE, Ewers BE, Phillips N, Schäfer KVR (1999) Survey and synthesis of intra-and interspecific variation in stomatal sensitivity to vapour pressure deficit. Plant Cell Environ 22:1515–1526.

Pataki DE, Oren R (2003) Species differences in stomatal control of water loss at the canopy scale in a mature bottomland deciduous forest. Adv Water Res 26:1267–1278.

Penman H (1948) Natural evaporation from open water, bare soil and grass. Proc R Soc Lond Ser A 193:120–145.

Phillips N, Oren R (1998) A comparison of daily representations of canopy conductance based on two conditional time-averaging methods and the dependence of daily conductance on environmental factors. Ann Sci For 55:217–235.

Phillips N, Oren R, Zimmermann R (1996) Radial patterns of xylem sap flow in non-, diffuse-and ring-porous tree species. Plant Cell Environ 19:983–990.

Priyadarshan PM (2003) Breeding *Hevea brasiliensis* for environmental constraints. Adv Agron 79:351–400.

Priyadarshan PM (ed) (2011) Biology of *Hevea* rubber. CAB International, Wallingford, UK.

Qiu J (2009) Where the rubber meets the garden. Nature 457:246.

Ranasinghe M, Milburn J (1995) Xylem conduction and cavitation in *Hevea brasiliensis*. J Exp Bot 46:1693–1700.

Rao G, Rao P, Rajagopal R, Devakumar A, Vijayakumar K, Sethuraj M (1990) Influence of soil, plant and meteorological factors on water relations and yield in *Hevea brasiliensis*. Int J Biometeorol 34: 175–180.

Sangsing K, Kasemsap P, Thanisawanyangkura S, Sangkhasila K, Gohet E, Thaler P, Cochard H (2004) Xylem embolism and stomatal regulation in two rubber clones (*Hevea brasiliensis* Muell. Arg.). Trees Struct Funct 18:109–114.

Schäfer KVR, Oren R, Tenhunen JD (2000) The effect of tree height on crown level stomatal conductance. Plant Cell Environ 23:365–375.

SCW (2006) Atlas of Cambodia: national poverty and environment maps. Phnom Penh, Cambodia.

Senevirathna A, Stirling C, Rodrigo V (2003) Growth, photosynthetic performance and shade adaptation of rubber (*Hevea brasiliensis*) grown in natural shade. Tree Physiol 23:705–712.

Silpi U, Thaler P, Kasemsap P, Lacointe A, Chantuma A, Adam B, Gohet E, Thaniswanyankura S, Améglio T (2006) Effect of tapping activity on the dynamics of radial growth of *Hevea brasiliensis* trees. Tree Physiol 26:1579–1587.

Simien A, Penot E (2011) Current evolution of smallholder rubber-based farming systems in southern Thailand. J Sustain For 30:247–260.

Snyder W, Wan Z, Zhang Y, Feng Y (1998) Classification-based emissivity for land surface temperature measurement from space. Int J Remote Sens 19:2753–2774.

Tan ZH, Zhang YP, Song QH et al. (2011) Rubber plantations act as water pumps in tropical China. Geophys Res Lett 38:L24406.

Tanaka K, Yoshifuji N, Tanaka N, Shiraki K, Tantasirin C, Suzuki M (2009) Water budget and the consequent duration of canopy carbon gain in a teak plantation in a dry tropical region: analysis using a soil–plant–air continuum multilayer model. Ecol Model 220:1534–1543.

Tsujimoto K, Masumoto T, Mitsuno T (2008) Seasonal changes in radiation and evaporation implied from the diurnal distribution of rainfall in the lower Mekong. Hydrol Process 22:1257–1266.

Van Genuchten MTh (1980) A closed-form equation for predicting the hydraulic conductivity of unsaturated soils. Soil Sci Soc Am J 44: 892–898.

Vijayakumar KR, Dey SK, Chandrasekhar TR, Devakumar AS, Mohankrishna T, Sanjeeva Rao P, Sethuraj MR (1998) Irrigation requirement of rubber trees (*Hevea brasiliensis*) in the subhumid tropics. Agric Water Manage 35:245–259.

Wauters JB, Coudert S, Grallien E, Jonard M, Ponette Q (2008) Carbon stock in rubber tree plantations in Western Ghana and Mato Grosso (Brazil). For Ecol Manage 255:2347–2361.

Wilson KB, Hanson PJ, Mulhollond PJ, Baldocchi DD, Wullschleger SD (2001) A comparison of methods for determining forest evapotranspiration and its components: sap-flow, soil water budget, eddy covariance and catchments water balance. Agric For Meteorol 106: 153–168.

Wu ZL, Liu HM, Liu LY (2001) Rubber cultivation and sustainable development in Xishuangbanna, China. Int J Sustain Dev World Ecol 8:337–345.

Ziegler A, Fox J, Xu J (2009) The rubber juggernaut. Science 324:1024.